Structural and functional characterization of an egg-laying hormone signaling system in a lophotrochozoan – The pacific oyster (Crassostrea gigas)

Pascal Favrel, M.P. Dubos, B. Bernay, J. Pasquier, J. Schwartz, B. Lefranc, L. Mouret, G. Rivière, J. Leprince, A. Bondon

Structural and functional characterization of an egg-laying hormone signaling system in a lophotrochozoan – the Pacific oyster (*Crassostrea gigas*)

P. Favrel[1*], MP. Dubos[1], B. Bernay[2], J. Pasquier[1], J Schwartz[1], B. Lefranc[3], L. Mouret[4], G. Rivière[1], J. Leprince[3], A. Bondon[4]

[1] Université Caen Normandie, Normandie Univ., Sorbonne Universités, MNHN, UPMC, UA, CNRS 7208, IRD 207, Biologie des Organismes et Ecosystèmes Aquatiques (BOREA), CS14032, Esplanade de la Paix, 14032 Caen, Cedex 5, France.

[2] Université Caen Normandie Normandie Université, US EMERODE, PROTEOGEN Core Facility, Esplanade de la Paix, 14032 Caen, France

[3]Université Rouen Normandie, INSERM, Normandie Université, NorDic UMR1239, Laboratoire de Différenciation et Communication Neuroendocrine, Endocrine et Germinale, F-76000 Rouen, France.

[4] Université Rennes 1, CNRS, ISCR-UMR 6226, COrInt, F-35000 Rennes, France

[*]*Corresponding author*: pascal.favrel@unicaen.fr

Abstract.

The egg-laying hormones (ELHs) of gastropod mollusks were characterized more than forty years ago. Yet, they have remained little explored in other mollusks. To gain insights into the functionality of the ELH signaling system in a bivalve mollusk – the oyster *Crassostrea gigas*, this study investigates the processing of its ELH precursor (Cragi-ELH) by mass spectrometry. Some of the ELH mature peptides identified in this study were subsequently investigated by nuclear magnetic resonance and shown to adopt an extended alpha-helix structure in a micellar medium mimicking the plasma membrane. To further characterize the ELH signaling system in *C. gigas*, a G protein-coupled receptor phylogenetically related to ecdysozoan diuretic

hormone DH44 and corticotropin-releasing hormone (CRH) receptors named Cragi-ELHR was also characterized functionally and shown to be specifically activated by the two predicted mature ELH peptides and their N-terminal fragments. Both Cragi-ELH and Cragi-ELHR encoding genes were mostly expressed in the visceral ganglia (VG). Cragi-ELH expression was significantly increased in the VG of both fully mature male and female oysters at the spawning stage. When the oysters were submitted to a nutritional or hyposaline stress, no change in the expression of the ligand or receptor genes was recorded, except for Cragi-ELHR only during a mild acclimation episode to brackish water. These results suggest a role of Cragi-ELH signaling in the regulation of reproduction but not in mediating the stress response in our experimental conditions.

Keywords: Oyster, GPCR, egg-laying hormone, reproduction, stress

Highlights:

- Cragi-ELHs adopt an extended alpha-helix structure in a micellar medium
- Cragi-ELHs activate a receptor phylogenetically related to DH44 and CRH receptors
- Cragi-ELH expression supports a role in the regulation of reproduction

1. Introduction

The egg-laying hormones (ELHs) of gastropods were among the first neuropeptides to be functionally characterized in mollusks (Chiu et al., 1979; Ebberink et al., 1985). They are synthesized as large precursor proteins that generate a set of neuropeptides in addition to ELHs and whose release controls and coordinates egg-laying and associated behavioral events in this class of mollusks [3-5]. With the development of transcriptomic and peptidomic resources for a variety of mollusks and annelids, it has become clear that orthologs of ELH neuropeptides exist in most lophotrochozoan species (Conzelmann et al., 2013; Jékely, 2013; Mirabeau and Joly, 2013; Salzet et al., 1997; Stewart et al., 2014; Veenstra, 2010). Because lophotrochozoan

ELHs display structural homologies with ecdysozoan diuretic hormone 44 (DH44) and deuterostome corticotropin-releasing hormone (CRH) family members (CRH, urocortins1-3: Ucn1-3), the ancestor of these families of neuropeptides predated the split between the protostome and deuterostome lineages.

Both vertebrate CRH family peptides and ecdysozoan DH44 are key players of the physiological response or tolerance to stress (Cannell et al., 2016; Deussing and Chen, 2018) and are involved in the regulation of a variety of physiological functions including feeding-associated processes (Cannell et al., 2016; Czimmer and Tache, 2017; Dus et al., 2015; Stengel and Taché, 2014; van Wielendaele et al., 2012), immunity (Lee et al., 2023), reproduction (van Wielendaele et al., 2012), body fluid secretion in *Drosophila* (Cabrero et al., 2002) and the renal function (Devetzis et al., 2013). Among Lophotrochozoa, besides gastropod ELHs, only a first insight into the physiological role of ELH as an egg-laying (spawning) hormone had been provided so far – in the Sydney rock oyster (*Saccostrea glomerata*) (In et al., 2016). Interestingly, a recent phylogenetic analysis showed that gastropod ELH sequences segregate apart from the clade including non-gastropod mollusk, annelid and nemertean counterparts (De Oliveira et al., 2019). This singular clustering of gastropod ELHs raises the prospect that they could have acquired specialized functions in relation with reproduction more recently throughout the evolution of mollusks. To gain insights into the functional involvement and the evolution of ELH signaling in mollusks, the present study characterizes functionally an ELH receptor for the first time in a Lophotrochozoan, and investigates the specific tissue-dependent, temporal and environment-induced expression of the genes encoding the components of the ELH signaling system in a bivalve mollusk – the oyster *Crassostrea gigas*.

2. Material and methods.

2.1. Animals and tissue sampling

Two-year old adult oysters *Crassostrea gigas* (Thunberg 1793), purchased from a local farm (Normandy, France), were used for peptide characterization and transcription analyses. Adult tissues, mantle, mantle edges, gills, labial palps, digestive gland, gonad (mix of all stages), heart, adductor muscle and the visceral ganglia (VG) were carefully dissected-out.

A one-year sampling of animals was undertaken to collect gonads and VG at different stages of reproduction. Oysters were collected and their gonads and VG were immediately dissected. VG and gonadal tissues were sampled for each individual, frozen in liquid nitrogen and stored at -80°C. A part of each gonad sample was also fixed for histological analysis. Gonadal development stage and sex were determined by histological methods according to the 4 stages previously described (Rodet et al., 2005): stage 0 corresponding to the resting undifferentiated stage with very few germinal stem cells; stage 1 corresponding to the gonial multiplication stage with poorly developed tubules surrounded by a large matrix of vesicular connective tissue (VTC); stage 2 corresponding to the maturation stage with tubule development and VCT starting to regress, with vitellogenesis occurring in females and all the cells of the germline can be observed in males (from spermatogonia to spermatozoa); stage 3 corresponding to sexual maturity with tubules full of mature germinal cells.

The effect of trophic conditions was investigated on one-year-old adult oysters reared in water tanks either in absence of food or in presence of *Isochrysis galbana* (clone T-Iso) maintained at a concentration of 6 million of cells/mL during 4 weeks. To study the influence of osmotic conditions, oysters were transferred from seawater (33‰) to brackish water (8‰) at 17°C by addition of distilled water once in the sea water tank (Acute stress) or by diluting the sea water with a continuous flow (0.5 Lh^{-1}) of distilled water during 3 days (Mild stress). To prevent the closure of the shell, a wedge was inserted between the valves before applying the stress. VG were sampled and frozen after 12 h of incubation of the oysters in brackish water at the final salinity.

2.2. Mass spectrometry characterization of oyster endogenous ELH peptides.

Peptide extraction: Fifteen VG, frozen and crushed in liquid nitrogen, were extracted in acetonitrile/water (90/10 v/v) 0.1% TFA for 30 minutes at 4°C. After centrifugation for 20 minutes at 15 000 g at 4°C, supernatant was concentrated on C18 Sep-Pak cartridges. Half of the recovered peptide sample was reduced with 100 mM DTT at 55 °C for 60 min and alkylated with 50 mM iodoacetamide at 55 °C for 45 min. Both mature or reduced/alkylated peptides were analyzed by mass spectrometry

For nano-LC fragmentation, peptide samples were first desalted and concentrated onto a µC18 Omix (Agilent) column before analysis. The chromatography step was performed on a NanoElute (Bruker Daltonics) ultra-high-pressure nano flow chromatography system. Approximatively 200ng of each peptide sample were concentrated onto a C18 pepmap 100 (5mm x 300µm i.d.) precolumn (Thermo Scientific) and separated at 50°C onto a reversed phase Reprosil column (25cm x 75µm i.d.) packed with 1.6µm C18 coated porous silica beads (Ionopticks). Mobile phases consisted of 0.1% formic acid, 99.9% water (v/v) (A) and 0.1% formic acid in 99.9% ACN (v/v) (B). The nanoflow rate was set at 300 nL/min, and the gradient profile was as follows: from 2 to 15% B within 15 min, followed by an increase to 25% B within 15 min and further to 35% within 12 min, followed by a washing step at 95% B and reequilibration.

MS experiments were carried out on an TIMS-TOF pro mass spectrometer (Bruker Daltonics) with a modified nano electrospray ion source (CaptiveSpray, Bruker Daltonics). A 1400 spray voltage with a capillary temperature of 180°C was typically employed for ionizing. MS spectra were acquired in the positive mode in the mass range from 100 to 1700 m/z. In the experiments described herein, the mass spectrometer was operated in PASEF mode without exclusion of single charged peptides. A number of 10 PASEF MS/MS scans was performed during 1.25 seconds from charge range 2-5 and the 1/K0 range 0.75-1.25.

Database searching was performed using the Peaks X+ software and a neuropeptide database comprising all known neuropeptide precursors from *C. gigas*. The variable modifications allowed were as follows: Carbamidomethylation (Cys residue), C-terminal amidation, Pyro-glutamination (Gln residue) and oxidation (Met residue). "No Enzyme" was selected. Mass accuracy was set to 20 ppm and 0.05 Da for MS and MS/MS mode, respectively. Data were filtering according to an FDR of 1%.

2.3. **Peptide synthesis**

2.3.1. Chemical Reagents.

All Fmoc amino acid residues, O-benzotriazol-1-yl-*N,N,N',N'*-tetramethyluronium hexafluorophosphate (HBTU), preloaded 4-hydroxymethyl-phenoxymethyl-copolystyrene-1%-divinylbenzene resins (HMP) and Rink amide 4-methylbenzhydrylamine (MBHA) resin were purchased from Novabiochem (Fontenay sous Bois, France) or IRIS Biotech (Marktredwitz, Germany). *N*,*N*-Diisopropylethylamine (DIEA), piperidine, trifluoroacetic acid (TFA), triisopropylsilane (TIS), tert-butylmethylether (TBME) were supplied from Sigma-Aldrich (Saint-Quentin-Fallavier, France). *N*-methylpyrrolidone (NMP), dimethylformamide (DMF), dichloromethane (DCM) and acetonitrile were from Fisher Scientific (Illkirch, France).

2.3.2. Peptide Synthesis.

Cragi-ELH1, Cragi-ELH1a, Cragi-ELH1b, Cragi-ELH1c, Cragi-ELH1$_{23\text{-}40}$, Cragi-ELH2, Cragi-ELH2a and Cragi-ELH2b were synthesized by Fmoc solid phase methodology on a Liberty microwave assisted automated peptide synthesizer (CEM, Saclay, France) using the standard manufacturer's procedures at 0.1 mmol scale as previously described (Touchard et al., 2020). All Fmoc-amino acids (0.5 mmol, 5 eq.) were coupled on preloaded HMP resin (ELH1a and ELH1c) or Rink amide resin (ELH1, ELH1b, ELH1$_{23\text{-}40}$, ELH2, ELH2a and ELH2b), by *in situ* activation with HBTU (0.5 mmol, 5 eq.) and DIEA (1 mmol, 10 eq.) before Fmoc removal

with 20% piperidine in DMF. After completion of the chain assembly, peptides were deprotected and cleaved from the resin by adding 10 mL of an ice-cold mixture of TFA/TIS/H_2O (9.5:0.25:0.25, v/v/v) and agitating for 3 hours at room temperature. After precipitation in TBME followed by centrifugation (4500 rpm, 15 min), the crude peptides were purified by reversed-phase HPLC (Gilson, Villiers le Bel, France) on a 21.2 x 250 mm Jupiter C18 (5 µm, 300 Å) column (Phenomenex, Le Pecq, France) using a linear gradient (10-60% or 20-50% over 45 min) of acetonitrile/TFA (99.9:0.1) at a flow rate of 10 mL/min. Peptides were then characterized by MALDI-TOF mass spectrometry on a ultrafleXtreme (Bruker, Strasbourg, France) in the reflectron mode using α-cyano-4-hydroxycinnamic acid as a matrix. Analytical RP-HPLC, performed on a 4.6 x 250 mm Jupiter C18 (5 µm, 300 Å) column, indicated that the purity of the peptides was > 99.9%.

with a 5 mm TCI cryoprobe (1H, 13C, 15N). Homonuclear 2-D spectra DQF-COSY, TOCSY and ROESY or

2.4. NMR and structure determination

2.4.1. NMR measurements

The nuclear magnetic resonance (NMR) samples contained 1-3 mM of peptide Cragi-ELH1a or Cragi-ELH2 dissolved in water or in presence of deuterated dodecylphosphocholine (DPC) micelles (125 mM). All spectra were recorded on a Bruker Avance 500 spectrometer equipped with a 5 mm TCI cryoprobe (1H, 13C, 15N). Homonuclear 2-D spectra - DQF-COSY, TOCSY and ROESY or NOESY were typically recorded using standard Bruker sequences in sensitive mode using the States-TPPI method. NOESY or ROESY spectra were acquired with 8 scans, 8 spectra were summed leading to less t1 noise as recently reported (Mo et al., 2017). Typical spectra were acquired using matrices of 4096 x 320-600 zero filled in F1 to 2K x 1K after apodization with shifted sine-square multiplication in both domains. Spectra were processed with Topspin software (Bruker).

2.4.2 Structure calculations

^{1}H chemical shifts were assigned according to classical sequential assignment procedure. NOE cross-peaks were integrated and assigned within the CcpNmr (Vranken et al., 2005) and NMR View software (Johnson, 2004). The volumes of NOE peaks between methylene pair protons were used as reference of 1.8 Å. Structure calculations were performed with AMBER 17 (Case et al., 2005) in two stages: cooking and simulated annealing in explicit solvent. The cooking stage was performed at 1000 K to generate 100 initial random structures. Simulated annealing calculations were carried during 20 ps (20000 steps, 1 fs long). First, the temperature was risen quickly and was maintained at 1000 K for the first 5000 steps, then the system was cooled gradually from 1000 K to 100 K from step 5001 to 18000 and finally the temperature was brought to 0 K during the 2000 remaining steps. For the 3000 first steps, the force constant of the distance restraints was increased gradually from 2.0 kcal.mol^{-1}.Å to 20 kcal.mol^{-1}.Å. For the rest of the simulation (step 3001 to 20000), the force constant is kept at 20 kcal.mol^{-1}.Å. The 20 lowest energy structures with no violations > 0.3 Å were considered as representative of the compound structure. All the dihedral angles ϕ and ψ belonged to the allowed regions of the Ramachandran plot. The representation and quantitative analysis were carried out using MOLMOL (Koradi et al., 1996).

2.5 *In silico* analyses

Multiple sequence alignment was performed using Clustal Omega (Sievers et al., 2011). Seaview (Gouy et al., 2010) was used for selecting the conserved protein regions and for manual correction of the alignment. PhyML was used for generating the trees. The reliability of the inferred trees was estimated by applying the bootstrap procedure with 1000 replications. FigTree (http://tree.bio.ed.ac.uk/software/figtree/) was used to draw the tree.

2.6 Pharmacological characterization of Cragi-ELHR

2.6.1 Molecular cloning and transfection of mammalian cells

The CDS of Cragi-ELHR (XP_034310400.1) was amplified by PCR using the transcript specific sense primer (5′-CACCATGTATAACCTGACGGACTATC-3′) harboring a Kozak consensus sequence and the antisense primer (5'-TTACAACATTTTCTCCGATTCTAGTCC-3′). Ten nanograms of plasmid DNA (Pal 17.3 vector, Evrogen, Russia) from a *C. gigas* "all developmental stages and adult central nervous system" normalized cDNA library (Fleury et al., 2009) was used as template. PCR was carried-out in a 50 µl reaction volume containing 1.5 mM $MgCl_2$, 200 mM dNTPs, 1 mM each of the primer couples, 1.25 units of GoTaq® polymerase and the appropriate buffer (Promega, Madison, WI, USA) in nuclease-free water. Samples were subjected to the following cycling parameters (95 °C, 2 min; 30 cycles of: 95 °C-45 s, 60°C-30 s, 72 °C-1 min, followed by 5 min at 72 °C).

The resulting PCR product was directionally cloned into the eukaryotic expression vector pTARGET (Promega) and the correct insertion confirmed by Sanger sequencing.

Human Embryonic Kidney (HEK293T) cells were transiently co-transfected with the Cragi-ELHR and pGloSensor™ - 22F cAMP (Promega) constructs using Fugene HD (Promega) according to the manufacturer's instructions. Cells for negative control experiments were transfected with an empty pcDNA3.1 and pGloSensor™ - 22F cAMP plasmids.

2.6.2 cAMP luminescence assay

Cragi-ELHR transfected HEK293 T cells were incubated with Glosensor cAMP reagent (4% final concentration in the medium) (Promega) for 2 hours at room temperature prior to the injection of the candidate ligands. The peptides to be tested were diluted at 5 times their final concentration in 20mM HEPES in Hank's balanced salt solution pH 7.3 and distributed in a 96-well plate. 25µL of the different peptide solutions were injected in the wells containing the cells. cAMP luminescence response was measured for 30 min after injection using a FLEX station 3 (Molecular Devices) at room temperature. Data were analyzed using SoftMax Pro

(Molecular Devices). Candidate peptide ligands were first tested in triplicate at a final concentration of 10^{-5} M then at different peptide concentrations. Concentration–response measurements of activating ligands were conducted in triplicate and for at least three independent experiments.

2.7 Reverse transcription and quantitative PCR

RT-qPCR analysis was performed using the CFX96™ Real-Time PCR Detection System (Bio-Rad, Hercules, CA, USA). Total RNA was isolated from adult tissues using Tri-Reagent (Sigma-Aldrich) according to the manufacturer's instructions. Recovered RNA was then further purified on Nucleospin RNAII columns (Macherey-Nagel). After treatment for 20 min at 37 °C with 1 U of DNase I (Sigma) to prevent genomic DNA contamination, 1 µg of total RNA was reverse transcribed using 1 µg of random hexanucleotide primers (Promega), 0.5 mM dNTPs and 200 U MMuLV Reverse Transcriptase (Promega) at 37 °C for 1 h in the appropriate buffer. The reaction was stopped by incubation at 70 °C for 10 min. The GoTaq® qPCR Master Mix (Promega) was used for real time monitoring of amplification (5 ng of cDNA template, 40 cycles: 95 °C/15s, 60 °C/15 s) with transcript specific primers for Cragi-ELH QF (5'-GTTCCGATACGGCAAAAGAA -3') and QR (5'- AATCAAGGGCGTTTGATCTG -3') and for Cragi-ELHR QF2 (5'- GGTCCCAATCGTTGCAAATCAA- 3') and QR2 (5' - CCCTCAACAAGCATCCAGAAGA-3') as forward (QF) and reverse (QR) primers respectively. Accurate amplification of the target amplicon was checked by performing a melting curve. A parallel amplification of *C. gigas* Elongation Factor1α (EF1α) QS-Cg-EF1α (5'-ACCACCCTGGTGAGATCAAG-3') and QA-Cg-EF1α (5'-ACGACGATCGCATTTCTCTT-3') transcript (BAD15289) was carried out to normalize the expression data of the analyzed transcripts. EF1α was used as a reliable normalization gene as no significant difference ($p < 0.05$) of Ct values was observed between the different samples

compared. Coefficient of variation of EF1α was less than 5% for all the tissue samples and experimental conditions. Thus, the relative level of expression of the target gene was calculated by using the following formula: $N = 2^{(Ct\ Cragi\text{-}EF1\alpha - Ct\ target\ cDNA)}$. The PCR amplification efficiency ($E = 10^{(-1/slope)}$) for each primer pair was determined by linear regression analysis of a dilution series to ensure that E ranged from 1.98 to 2.02.

2.8 Statistical analysis

Gene expression levels between different tissues and between samples at different reproduction stages were compared using one-way ANOVA followed by a Tukey post hoc test. Expression levels between animals in different feeding or salinity conditions were compared using an unpaired Student's t test. Significance was set at $p < 0.05$.

3 Results.

3.1 Molecular processing of Cragi-ELH precursor.

The sequence of the precursor encoding *C. gigas* ELH (Cragi-ELH) described previously (Stewart et al., 2014) harbors two predicted neurohormones Cragi-ELH1 and Cragi-ELH2. Alignment of the predicted two oyster mature peptide sequences demonstrates sequence similarity in terms of peptide length, C-terminal amidation and, especially in the N-terminal and C-terminal regions, the occurrence of conserved amino acids at similar positions with vertebrate corticotropin releasing hormone (CRH), insect diuretic hormone (DH 44) and Lophotrochozoan egg-laying hormones (ELH) (Fig. 1). To determine the processing of Cragi-ELH precursor, mass spectrometric methods were used. Analysis of VG extracts allowed the detection of many mature peptides overlapping the entire precursor protein (Fig. 2A, Suppl Fig.1, iProX database IPX0007327001). A peptide corresponding to the predicted full length Cragi-ELH1 could not be detected whilst the corresponding peptides predicted to be generated

owing to the presence of prohormone convertase processing sites were all unambiguously detected (Cragi-ELH1a: GRLSLTADLRSLARMLEAH, monoisotopic mass of m/z 528.2821 [4+], Cragi-ELH1b: FIASRFPYDSI m/z 658.34 [2+], Cragi-ELH1c: LFRYamide m/z 597.35 [1+]). For Cragi-ELH2, a single peptide of monoisotopic mass of m/z 845.4257 [5+], corresponding to the full-length sequence could be detected. In contrast, despite the presence of a monobasic putative processing site, no Cragi-ELH2 processed peptides could be detected.

3.2 Structure determination of Cragi-ELH peptides by NMR

The NMR analysis of ELH1a, as the longest processed peptide from predicted ELH1 sequence and ELH2 in presence of deuterated DPC was performed using the sequential assignment strategy (Wüthrich, 1986). As presented in supplementary tables 1 and 2, the complete chemical shift assignment of ELH1a was successfully performed whereas severe overlapping prevented the full assignment of ELH2. The three-dimensional structure of peptide ELH1a in DPC micelles was solved. The superposition of the 18 lowest energy conformers, fitted on segment 4-17 backbone atoms is presented in Fig. 2B. Summary of the refinement statistics are given (Suppl. table 3). An alpha helix is clearly defined between the residues 4 to 17. Incomplete assignment of ELH2 prevents the structure determination, however the NOE connectivity pattern is also characteristic of a helical structuration of the ELH2 peptide in DPC micelles with numerous inter residue i - i+3 connectivities between the residues 4-19 (Suppl. Fig. 2).

3.3 Characterization of Cragi-ELHR

A BLAST search using the *Drosophila* DH44 Receptor 1 (DH44R1: AAF58250.1) sequence in the Gigaton database (Riviere et al., 2015) allowed the identification of a full-length transcript (CHOYP_CRHR.1.2) encoding a seven transmembrane domain protein typical of a GPCR (Suppl. Fig. 3). Alignment of the oyster receptor named Egg-laying Hormone Receptor (Cragi-ELHR) with vertebrate and protostome GPCRs highlights its high degree of homology

with functionally characterized insect DH44Rs, lophotrochozoan putative DH44/CRHRs and vertebrate CRHRs (Suppl. Table 4 and Suppl. Fig. 4). A phylogenetic analysis showed that all lophotrochozoan receptors form a single clade and were phylogenetically related to vertebrate CRHRs and Ecdysozoan DH44Rs (Fig. 3). Transiently transfected HEK293T cells expressing Cragi-ELHR were challenged with Cragi-ELH1 and Cragi-ELH2 as well as with all their predicted or characterized processed peptides (Cragi-ELH1a, Cragi-ELH1b, Cragi-ELH1c, Cragi-ELH123-40, Cragi-ELH2a and Cragi-ELH2b) at a single concentration of 10^{-5}M. Both Cragi-ELH1 and Cragi-ELH2 activated Cragi-ELHR resulting in the activation of the adenylyl-mediated cAMP transduction pathway. Only N-terminal peptides of both Cragi-ELH1 (Cragi-ELH1a) and Cragi-ELH2 (Cragi-ELH2a) were efficient in activating Cragi-ELHR though C-terminal and central peptides were not (Fig.4A). Thus, a dose-dependent activation of Cragi-ELHR was investigated using the active peptides. Both Cragi-ELH1 and Cragi-ELH2 elicited a gradual response with an EC50 of respectively 26.2 ± 3.2 nM and 81.3 ± 8.9 nM whilst ELH1a and ELH2a showed an EC50 of 2.88 ± 0.76µM and of 3.11 ± 1.29 µM respectively (Fig.4B). Only micromolar concentrations of ELH1 and ELH2 triggered the phospholipase Cβ-mediated calcium transduction pathway (data not shown)

3.4 Gene expression of Cragi-ELHR and Cragi-ELH.

The expression of Cragi-ELHR and Cragi-ELH precursor transcripts was investigated by RT-qPCR in several adult tissues, in VG and gonads during reproduction and in VG of animals exposed to different stresses (Supplementary table 5). Both Cragi-ELHR and Cragi-ELH precursor genes were majorly expressed in the VG and at very much lower levels in most adult tissues (Fig. 5A and B). During a cycle of reproduction, no significant change in expression of Cragi-ELHR was observed both in male and female VG or gonads (Fig. 5C and D). In contrast, a significantly higher expression of Cragi-ELH precursor gene was noticed only in VG at stage 3 in both males and females (Fig. 5C). Given the implication of vertebrate CRH in mediating

stress, two stress conditions were applied to oysters. The first stress was to starve animals for a period of four weeks. In these conditions, no significant change of expression of Cragi-ELH or Cragi-ELHR transcripts was observed in the VG of starved animals as compared to VG of fed animals (Fig. 6A and B). The second stress was to expose oysters to brackish water either suddenly (acute stress) or by progressively changing the salinity over a period of three days (mild stress). Only Cragi-ELHR gene expression was found to be significantly stimulated in mild stress conditions in the VG whilst no change was found for Cragi-ELH transcripts for both stresses in the VG (Fig. 6C and D).

4 Discussion

The present work describes the functional characterization of a lophotrochozoan G protein-coupled receptor (GPCR) phylogenetically related to insect DH44Rs and vertebrate CRH family member receptors. Our phylogenetic analysis is congruent with previous studies (Cardoso et al., 2014) and suggests that mollusk and annelid receptors are more similar to chordate CRHRs than to insect DH44Rs. Interestingly, the receptors obviously cluster according to the animal phylogeny, whereas among the ligands, gastropod ELHs segregate apart and form an independent and specific clade beside the group gathering the remaining mollusk and lophotrochozoan ELH/DH44 sequences (De Oliveira et al., 2019). This suggests a specific evolution of gastropod ligands, potentially in association with their specific role in the control of reproductive behavioral processes (Scheller et al., 1982; Vreugdenhil et al., 1988). Among mollusks, cephalopods also display a complex pattern of reproductive behaviors (von Boletzky, 1983) involving a variety of neuropeptides (Henry et al., 1999; Zatylny-Gaudin et al., 2016; Zatylny et al., 2000). However, no ELH-related peptide was identified from the neuro-transcriptome and the neuropeptidome of spawning cuttlefish (*Sepia officinalis*) (Zatylny-Gaudin et al., 2016). It has been suggested that the ELH-encoding gene may have been lost in cephalopods (De Oliveira et al., 2019). The present study clearly shows the existence of an

ELHR in the cephalopod *Octopus bimaculoides*, noticeably phylogenetically distant from the other lophotrochozoan receptors. This possibly indicates that it binds peptide ligands divergent from their lophotrochozoan counterparts.

In the same way as other bivalve precursors (Stewart et al., 2014; Zhang et al., 2018), the Cragi-ELH precursor potentially generates two homologous ELHs (Cragi-ELH1 and Cragi-ELH2) of 40 and 38 amino acids, respectively (Stewart et al., 2014). Both peptides specifically activate Cragi-ELHR at nanomolar concentrations, as observed for insect DH44Rs and vertebrate CRHRs and their respective ligands (Chen et al., 1993; Hector et al., 2009; Johnson et al., 2005; Liaw et al., 1996). Cragi-ELHR increased cAMP levels upon activation, as most receptors of this family do (Chen et al., 1993; Hector et al., 2009; Johnson et al., 2005; Liaw et al., 1996), but which are otherwise promiscuous as to the Gα type they activate (Grammatopoulos, 2012). In our experimental conditions, only micromolar concentrations of Cragi-ELH1 and Cragi-ELH2 increased intracellular calcium, as found for DH44R1 in *Drosophila* (Johnson et al., 2004). Structure-activity relationships were examined, and demonstrated that like vertebrate CRHs (Deussing and Chen, 2018), synthetic N-terminal fragments of Cragi-ELH1 and Cragi-ELH2 were efficient to activate Cragi-ELHR, though with less potency than their respective full-length forms. Both the N- and C-terminal moieties of Cragi-ELHs display very high conservation with other CRH/DH44/ELH peptides. This suggests that, as in vertebrate CRHs, the N-terminal part of the ligand is crucial for receptor binding and activation, although the C-terminal part would be responsible for the affinity and specificity of the ligand (Deussing and Chen, 2018). Although the conformation of oyster ELHs had been predicted (Stewart et al., 2014), their high-resolution structure was determined by NMR in this study. From a structural point of view, there was no defined structure of the ELH1a and ELH2 peptides in water, as often encountered with small peptides. However, an extended alpha helix was found in a micellar medium after molecular modeling using NMR constraints. Also observed in human

and rat CRHs (Spyroulias et al., 2002) and more generally in Class B GPCR ligands (Neumann et al., 2008), such a structuring of Cragi-ELH1a and Cragi-ELH2 in close proximity to the membrane is consistent with the idea that peptides can adopt a helical structure in the vicinity of their membrane receptors.

It was somewhat intriguing to observe that Cragi-ELH1 was much more potent than Cragi-ELH2 to activate Cragi-ELHR. Yet, unlike Cragi-ELH2, Cragi-ELH1 does not seem to exist as a molecular entity in oyster: it is processed into three unrelated peptides (ELH1a, ELH1b and ELH1c). We cannot exclude the possibility that Cragi-ELH1 was not detected by MS due to an inappropriate extraction procedure or poor ionization of the peptide. However, we think this is unlikely because Cragi-ELH1 cleavage peptides have been easily identified by MS, which means that Cragi-ELH1 occurs in rather small amounts if it does exist. As a result, Cragi-ELH2 appears as the main activator of the ELH signaling system in *C. gigas* given the poor potency of ELH1a in activating Cragi-ELHR. Potency differences between Cragi-ELH2 and Cragi-ELH1a may reflect respective roles as a neurohormone and a neurotransmitter. Nevertheless, apart from Cragi-ELH1a, the other two neuropeptides generated by the processing of Cragi-ELH1 constitute potential biologically active factors regulating target tissues *via* distinct receptors. The processing of Cragi-ELH1 is somewhat reminiscent of that of *Aplysia californica* ELH and *Lymnaea stagnalis* CDCH precursors: multiple short peptides (α/β BCPs, α/β CDCPs) are generated that play a role as neurotransmitters (Scheller et al., 1983) and control the activity of various target neurons implied in the reproductive behavior of *L. stagnalis* (Koene, 2010). Out of the three neuropeptides generated from the processing of Cragi-ELH1, the C-terminal tetrapeptide LFRYamide (Cragi-ELH1c) exhibited a sequence identical to the C-terminal sequence of Cragi-LXRYamide (Réalis-Doyelle et al., 2021), and its structure clearly resembled that of the LFRFamide family of neuropeptides identified in *C. gigas* (Bigot et al., 2014). In agreement with a previous work (Réalis-Doyelle et al., 2021), the present study

shows that Cragi-ELH gene expression peaks in the VG of reproductively mature male and female oysters. Interestingly, the expression of the Cragi-LXRYamide-encoding gene increased in parallel to that of the Cragi-ELH-encoding gene in the VGs of reproductively mature oysters (Réalis-Doyelle et al., 2021). In addition, LFRFamide signaling regulates reproduction and feeding processes in mollusks (Bigot et al., 2014; Hoek et al., 2005). Thus, although encoded by different genes, these closely structurally related neuropeptides may synergistically activate the same receptor and contribute to regulate reproduction- and feeding-associated functions in oysters. The significant increased expression of Cragi-ELH in the VGs of mature oysters suggests a role in the regulation of reproduction. However, considering the low and stable expression of Cragi-ELHR in oyster gonads during a reproductive cycle, it is not clear whether Cragi-ELH signaling is directly involved in spawning. The highest levels of expression of Cragi-ELHR and Cragi-ELH in the VGs compared to other adult tissues rather suggest a reproduction-associated neuroregulatory role in the central nervous system. Cragi-ELH signaling is likely not involved in the regulation of feeding, as no significant change was recorded in the expression of ELH receptor- and ligand-encoding genes during a nutritional stress. This is in contrast with the reported role of DH44 in inducing satiety in the desert locust *Schistocerca gregaria* (van Wielendaele et al., 2012). Given the major role of CRH and DH44 in mediating the stress response and the regulation of osmolarity, it was rational to investigate the possible role of Cragi-ELH signaling during a hypoosmotic stress – a common environmental pressure experienced by oysters in estuaries (Guo et al., 2015). Cragi-ELH tended to increase in the VG following a mild or acute hypoosmotic stress, but these changes were not statistically significant, whereas Cragi-ELHR increased significantly in mild stress conditions. Complementary experiments should be carried out on animals exposed to other stress conditions or other stressors (i.e., temperature or air exposure), but our results suggest that Cragi-ELH signaling does not represent a key neuroendocrine pathway of the stress

response or osmotic regulation in *C. gigas*. In contrast, decreased expression of the CCAP signaling components has been evidenced in the gills of oyster (Realis-Doyelle et al., 2021) in similar mild hyposaline conditions. Conversely, the two distinct calcitonin (CT) signaling systems of *C. gigas* showed opposite responses in lower saline concentration conditions: CT1b/CTR expression decreased, whereas CT2/CTR2 expression increased (Schwartz et al., 2019).

5 Conclusion

An ELH signaling system was characterized for the first time in a lophotrochozoan species. This signaling system is evolutionarily related to the vertebrate CRH and arthropod DH44 signaling systems. The involvement of ELH signaling in the regulation of reproduction-related functions in oysters is very likely, while its involvement in mediating the stress response remains doubtful.

6 References

Bigot, L., Beets, I., Dubos, M.-P., Boudry, P., Schoofs, L., Favrel, P., 2014. Functional characterization of a short neuropeptide F-related receptor in a lophotrochozoan, the mollusk *Crassostrea gigas*. J. Exp. Biol. 217, 2974–2982. https://doi.org/10.1242/jeb.104067

Cabrero, P., Radford, J.C., Broderick, K.E., Costes, L., Veenstra, J.A., Spana, E.P., Davies, S.A., Dow, J.A.T., 2002. The Dh gene of *Drosophila melanogaster* encodes a diuretic peptide that acts through cyclic AMP. J. Exp. Biol. 205, 3799–3807. https://doi.org/10.1242/jeb.205.24.3799

Cannell, E., Dornan, A.J., Halberg, K.A., Terhzaz, S., Dow, J.A.T., Davies, S.A., 2016. The corticotropin-releasing factor-like diuretic hormone 44 (DH44) and kinin neuropeptides

449 modulate desiccation and starvation tolerance in *Drosophila melanogaster*. Peptides 80,
450 96–107. https://doi.org/10.1016/j.peptides.2016.02.004

451 Cardoso, J.C.R., Félix, R.C., Bergqvist, C.A., Larhammar, D., 2014. New insights into the
452 evolution of vertebrate CRH (corticotropin-releasing hormone) and invertebrate DH44
453 (diuretic hormone 44) receptors in metazoans. Gen. Comp. Endocrinol. 209, 162–170.
454 https://doi.org/10.1016/j.ygcen.2014.09.004

455 Case, D.., Cheatham, T.., Darden, T., Gohlke, H., Luo, R., Merz, K.., Onufriev, A., 2005. The
456 Amber biomolecular simulation programs. J Comput. Chem. 1668–1688.
457 https://doi.org/10.1002/jcc.20290

458 Chen, R., Lewis, K.A., Perrin, M.H., Vale, W.W., 1993. Expression cloning of a human
459 corticotropin-releasing-factor receptor. Proc. Natl. Acad. Sci. U. S. A. 90, 8967–8971.
460 https://doi.org/10.1073/pnas.90.19.8967

461 Chiu, A.Y., Hunkapiller, M.W., Heller, E., Stuart, D.K., Hood, L.E., Strumwasser, F., 1979.
462 Purification and primary structure of the neuropeptide egg-laying hormone of *Aplysia*
463 *californica*. Proc. Natl. Acad. Sci. U. S. A. 76, 6656–6660.
464 https://doi.org/10.1073/pnas.76.12.6656

465 Conzelmann, M., Williams, E.A., Krug, K., Franz-wachtel, M., Macek, B., 2013. The
466 neuropeptide complement of the marine annelid *Platynereis dumerilii*. BMC Genomics
467 14, 906.

468 Czimmer, J., Tache, Y., 2017. Peripheral Corticotropin Releasing Factor Signaling Inhibits
469 Gastric Emptying: Mechanisms of Action and Role in Stress-related Gastric Alterations
470 of Motor Function. Curr. Pharm. Des. 23, 4042–4047.

471 De Oliveira, A.L., Calcino, A., Wanninger, A., 2019. Extensive conservation of the

proneuropeptide and peptide prohormone complement in mollusks. Sci. Rep. 9, 1–17. https://doi.org/10.1038/s41598-019-40949-0

Deussing, J.M., Chen, A., 2018. The Corticotropin-Releasing Factor Family: Physiology of the Stress Response. Physiol. Rev. 98, 2225–2286. https://doi.org/10.1152/physrev.00042.2017

Devetzis, V., Zarogoulidis, P., Kakolyris, S., Vargemezis, V., Chatzaki, E., 2013. The corticotropin releasing factor system in the kidney: perspectives for novel therapeutic intervention in nephrology. Med res rev. 33, 847–872. https://doi.org/10.1002/med

Dus, M., Lai, J.S.Y., Gunapala, K.M., Min, S., Tayler, T.D., Hergarden, A.C., Geraud, E., Joseph, C.M., Suh, G.S.B., 2015. Nutrient Sensor in the Brain Directs the Action of the Brain-Gut Axis in *Drosophila*. Neuron 87, 139–151. https://doi.org/10.1016/j.neuron.2015.05.032

Ebberink, R.H.M., Van Loenhout, H., Geraerts, W.P.M., Joosse, J., 1985. Purification and amino acid sequence of the ovulation neurohormone of *Lymnaea stagnalis*. Proc. Natl. Acad. Sci. U. S. A. 82, 7767–7771. https://doi.org/10.1073/pnas.82.22.7767

Fleury, E., Huvet, A., Lelong, C., Lorgeril, J. De, Boulo, V., Gueguen, Y., Bachère, E., Tanguy, A., Moraga, D., Fabioux, C., Lindeque, P., Shaw, J., Reinhardt, R., Prunet, P., Davey, G., Lapègue, S., Sauvage, C., Corporeau, C., Moal, J., Gavory, F., Wincker, P., Moreews, F., Klopp, C., Mathieu, M., Boudry, P., Favrel, P., 2009. Generation and analysis of a 29 , 745 unique Expressed Sequence Tags from the Pacific oyster (*Crassostrea gigas*) assembled into a publicly accessible database : the GigasDatabase. BMC Genomics 15, 1–15. https://doi.org/10.1186/1471-2164-10-341

Gouy, M., Guindon, S., Gascuel, O., 2010. SeaView version 4: A multiplatform graphical user interface for sequence alignment and phylogenetic tree building. Mol. Biol. Evol. 27, 221–

4. https://doi.org/10.1093/molbev/msp259

Grammatopoulos, D.K., 2012. Insights into mechanisms of corticotropin-releasing hormone receptor signal transduction. Br. J. Pharmacol. 166, 85–97. https://doi.org/10.1111/j.1476-5381.2011.01631.x

Guo, X., He, Y., Zhang, L., Lelong, C., Jouaux, A., 2015. Immune and stress responses in oysters with insights on adaptation. Fish Shellfish Immunol. 46, 107–119. https://doi.org/10.1016/J.FSI.2015.05.018

Hector, C.E., Bretz, C.A., Zhao, Y., Johnson, E.C., 2009. Functional differences between two CRF-related diuretic hormone receptors in *Drosophila*. J. Exp. Biol. 212, 3142–3147. https://doi.org/10.1242/jeb.033175

Henry, J., Zatylny, C., Boucaud-Camou, E., 1999. Peptidergic control of egg-laying in the cephalopod *Sepia officinalis*: involvement of FMRFamide and FMRFamide-related peptides. Peptides 20, 1061–70.

Hoek, R.M., Li, K.W., van Minnen, J., Lodder, J.C., de Jong-Brink, M., Smit, A.B., van Kesteren, R.E., 2005. LFRFamides: a novel family of parasitation-induced -RFamide neuropeptides that inhibit the activity of neuroendocrine cells in *Lymnaea stagnalis*. J. Neurochem. 92, 1073–80. https://doi.org/10.1111/j.1471-4159.2004.02927.x

In, V. Van, Ntalamagka, N., O'Connor, W., Wang, T., Powell, D., Cummins, S.F., Elizur, A., 2016. Reproductive neuropeptides that stimulate spawning in the Sydney Rock Oyster (*Saccostrea glomerata*). Peptides 82, 109–119. https://doi.org/10.1016/j.peptides.2016.06.007

Jékely, G., 2013. Global view of the evolution and diversity of metazoan neuropeptide signaling. Proc Natl Acad Sci U S A 110, 8702–8707.

https://doi.org/10.1073/pnas.1221833110

Johnson, B.A., 2004. Protein NMR Techniques. Using NMRView to Visualize and Analyze the NMR Spectra of Macromolecules. Humana Press, New jersey.

Johnson, E.C., Bohn, L.B., Taghert, P.H., 2004. *Drosophila* CG8422 encodes a functional diuretic hormone receptor. J. Exp. Biol. 207, 743–748. https://doi.org/10.1242/jeb.00818

Johnson, E.C., Shafer, O.T., Trigg, J.S., Park, J., Schooley, D.A., Dow, J., Taghert, P.H., 2005. A novel diuretic hormone receptor in *Drosophila*: evidence for conservation of CGRP signaling. J. Exp. Biol. 208, 1239–1246. https://doi.org/10.1242/jeb.01529

Koene, J.M., 2010. Neuro-endocrine control of reproduction in hermaphroditic freshwater snails: mechanisms and evolution. Front. Behav. Neurosci. 4, 167. https://doi.org/10.3389/fnbeh.2010.00167

Koradi, R., Billeter, M., Wüthrich, K., 1996. MOLMOL: A program for display and analysis of macromolecular structures. J Mol. graph. 51–55. https://doi.org/10.1016/0263-7855(96)00009-4

Lee, G., Jang, H., Oh, Y., Oh, T., 2023. The role of diuretic hormones (DHs) and their receptors in *Drosophila*. BMB Rep 56, 5864. https://doi.org/10.5483/bmbrep.2023-0021

Liaw, C., Lovenberg, T., Barry, G., Oltersdorf, T., Grigoriadis, D., De Souza, E., 1996. Cloning and characterization of the human corticotropin-releasing factor-2 receptor complementary deoxyribonucleic acid. Endocrinology 137, 72–77.

Mirabeau, O., Joly, J., 2013. Molecular evolution of peptidergic signaling systems in bilaterians. Proc Natl Acad Sci U S A 110, 2028–2037. https://doi.org/10.1073/pnas.1219956110/-/DCSupplemental.www.pnas.org/cgi/doi/10.1073/pnas.1219956110

Mo, H., Harwood, J.., Yang, D., Post, C.., 2017. A simple method for NMR t1 noise suppression. J. Magn. Reson 276, 43–50. https://doi.org/10.1016/j.jmr.2016.12.014

Neumann, J.M., Couvineau, A., Murail, S., Lacapère, J.J., Jamin, N., Laburthe, M., 2008. Class-B GPCR activation: is ligand helix-capping the key? Trends Biochem. Sci. 33, 314–319. https://doi.org/10.1016/j.tibs.2008.05.001

Réalis-Doyelle, E., Schwartz, J., Cabau, C., Franc, L. Le, Bernay, B., Rivière, G., Klopp, C., Favrel, P., 2021. Transcriptome profiling of the pacific oyster *Crassostrea gigas* visceral ganglia over a reproduction cycle identifies novel regulatory peptides. Mar. Drugs 19. https://doi.org/10.3390/md19080452

Realis-Doyelle, E., Schwartz, J., Dubos, M.-P.P., Favrel, P., 2021. Molecular and physiological characterization of a crustacean cardioactive signaling system in a lophotrochozoan – the pacific oyster *(Crassostrea gigas)*: a role in reproduction and salinity acclimation. J Exp Biol 224, jeb241588. https://doi.org/10.1242/jeb.241588

Riviere, G., Klopp, C., Ibouniyamine, N., Huvet, A., Boudry, P., Favrel, P., 2015. GigaTON: an extensive publicly searchable database providing a new reference transcriptome in the pacific oyster *Crassostrea gigas*. BMC Bioinformatics 16, 401. https://doi.org/10.1186/s12859-015-0833-4

Rodet, F., Lelong, C., Dubos, M.-P., Costil, K., Favrel, P., 2005. Molecular cloning of a molluscan gonadotropin-releasing hormone receptor orthologue specifically expressed in the gonad. Biochim Biophys Acta 1730, 187–195. https://doi.org/10.1016/j.bbaexp.2005.05.012

Salzet, M., Verger-Bocquet, M., Vandenbulcke, F., Van Minnen, J., 1997. Leech egg-laying-like hormone: Structure, neuronal distribution and phylogeny. Mol. Brain Res. 49, 211–221. https://doi.org/10.1016/S0169-328X(97)00145-9

566 Scheller, R.H., Jackson, J.F., McAllister, L.B., Rothman, B.S., Mayeri, E., Axel, R., 1983. A
567 single gene encodes multiple neuropeptides mediating a stereotyped behavior. Cell 32, 7–
568 22. https://doi.org/10.1016/0092-8674(83)90492-0

569 Scheller, R.H., Jackson, J.F., McAllister, L.B., Schwartz, J.H., Kandel, E.R., Axel, R., 1982. A
570 family of genes that codes for ELH, a neuropeptide eliciting a stereotyped pattern of
571 behavior in *Aplysia*. Cell 28, 707–719. https://doi.org/10.1016/0092-8674(82)90050-2

572 Schwartz, J., Réalis-Doyelle, E., Dubos, M.P., Lefranc, B., Leprince, J., Favrel, P., 2019.
573 Characterization of an evolutionarily conserved calcitonin signalling system in a
574 lophotrochozoan, the Pacific oyster (*Crassostrea gigas*). J. Exp. Biol. 222.
575 https://doi.org/10.1242/jeb.201319

576 Sievers, F., Wilm, A., Dineen, D., Gibson, T.J., Karplus, K., Li, W., Lopez, R., McWilliam, H.,
577 Remmert, M., Söding, J., Thompson, J.D., Higgins, D.G., 2011. Fast, scalable generation
578 of high-quality protein multiple sequence alignments using Clustal Omega. Mol. Syst.
579 Biol. 7, 539. https://doi.org/10.1038/msb.2011.75

580 Spyroulias, G.A., Papazacharias, S., Pairas, G., Cordopatis, P., 2002. Monitoring the structural
581 consequences of Phe12 → D-Phe and Leu15 → Aib substitution in human/rat corticotropin
582 releasing hormone: Implications for design of CRH antagonists. Eur. J. Biochem. 269,
583 6009–6019. https://doi.org/10.1046/j.1432-1033.2002.03278.x

584 Stengel, A., Taché, Y., 2014. CRF and urocortin peptides as modulators of energy balance and
585 feeding behavior during stress. Front. Neurosci. 8, 1–10.
586 https://doi.org/10.3389/fnins.2014.00052

587 Stewart, M.J., Favrel, P., Rotgans, B.A., Wang, T., Zhao, M., Sohail, M., O'Connor, W.A.,
588 Elizur, A., Henry, J., Cummins, S.F., O'Connor, W.A., Elizur, A., Henry, J., Cummins,
589 S.F., 2014. Neuropeptides encoded by the genomes of the Akoya pearl oyster *Pinctata*

590 *fucata* and Pacific oyster *Crassostrea gigas*: a bioinformatic and peptidomic survey. BMC
591 Genomics 15, 840. https://doi.org/10.1186/1471-2164-15-840

592 Touchard, A., Aili, S.R., Téné, N., Barassé, V., Klopp, C., Dejean, A., Kini, R.M., Mrinalini,
593 Coquet, L., Jouenne, T., Lefranc, B., Leprince, J., Escoubas, P., Nicholson, G.M.,
594 Treilhou, M., Bonnafé, E., 2020. Venom Peptide Repertoire of the European Myrmicine
595 Ant *Manica rubida*: Identification of Insecticidal Toxins. J. Proteome Res. 19, 1800–1811.
596 https://doi.org/10.1021/acs.jproteome.0c00048

597 van Wielendaele, P., Dillen, S., Marchal, E., Badisco, L., Vanden Broeck, J., 2012. CRF-like
598 diuretic hormone negatively affects both feeding and reproduction in the desert locust,
599 *Schistocerca gregaria*. PLoS One 7. https://doi.org/10.1371/journal.pone.0031425

600 Veenstra, J. A, 2010. Neurohormones and neuropeptides encoded by the genome of *Lottia*
601 *gigantea*, with reference to other mollusks and insects. Gen. Comp. Endocrinol. 167, 86–
602 103. https://doi.org/10.1016/j.ygcen.2010.02.010

603 Von Boletzky, S., 1983. *Sepia officinalis*. In Cephalopod Life Cycles, in: Boyle, E. (Ed.), .
604 Academic Press, London, pp. 31–52.

605 Vranken, W., Boucher, W., Stevens, T.., Fogh, R.., Pajon, A., Llinas, M., Ulrich, E.., Markley,
606 J.., Ionides, J., Laue, E.., 2005. The CCPN data model for NMR spectroscopy:
607 Development of a software pipeline. Protein struct. funct. Bioinforma. 687–696.
608 https://doi.org/10.1002/prot.20449

609 Vreugdenhil, E., Jackson, J.F., Bouwmeester, T., Smit, A.B., Van Minnen, J., Van
610 Heerikhuizen, H., Klootwijk, J., Joosse, J., 1988. Isolation, characterization, and
611 evolutionary aspects of a cDNA clone encoding multiple neuropeptides involved in the
612 stereotyped egg-laying behavior of the freshwater snail *Lymnaea stagnalis*. J. Neurosci. 8,
613 4184–4191. https://doi.org/10.1523/jneurosci.08-11-04184.1988

Wüthrich, K., 1986. NMR of Proteins and Nucleic Acids. wiley, New York.

Zatylny-Gaudin, C., Cornet, V., Leduc, A., Zanuttini, B., Corre, E., Le Corguillé, G., Bernay, B., Garderes, J., Kraut, A., Couté, Y., Henry, J., 2016. Neuropeptidome of the cephalopod *Sepia officinalis*: identification, tissue mapping, and expression pattern of neuropeptides and neurohormones during egg laying. J. Proteome Res. 15, 48–67. https://doi.org/10.1021/acs.jproteome.5b00463

Zatylny, C., Gagnon, J., Boucaud-Camou, E., Henry, J., 2000. The SepOvotropin: a new ovarian peptide regulating oocyte transport in *Sepia officinalis*. Biochem Biophys Res Commun 276, 1013–1018.

Zhang, M., Wang, Y., Li, Y., Li, W., Li, R., Xie, X., Wang, S., Hu, X., Zhang, L., Bao, Z., 2018. Identification and characterization of neuropeptides by transcriptome and proteome analyses in a bivalve mollusc *Patinopecten yessoensis*. Front. Genet. 9, 197. https://doi.org/10.3389/fgene.2018.00197

Competing interests:

The authors declare no competing or financial interests

Fundings:

This work was supported by the ANR project NEMO (Agence Nationale de la Recherche 14CE02 0020) and by the Council of the Normandy Region (RIN ECUME: 18E01643-18P02383) to P. Favrel.

Credit authorship contribution statement:

PF, JL and AB designed the study; MPD, JP, JS, BB, LM, GR, JL and AB performed the experiments and analyzed, PF wrote the paper. All authors reviewed and edited the manuscript.

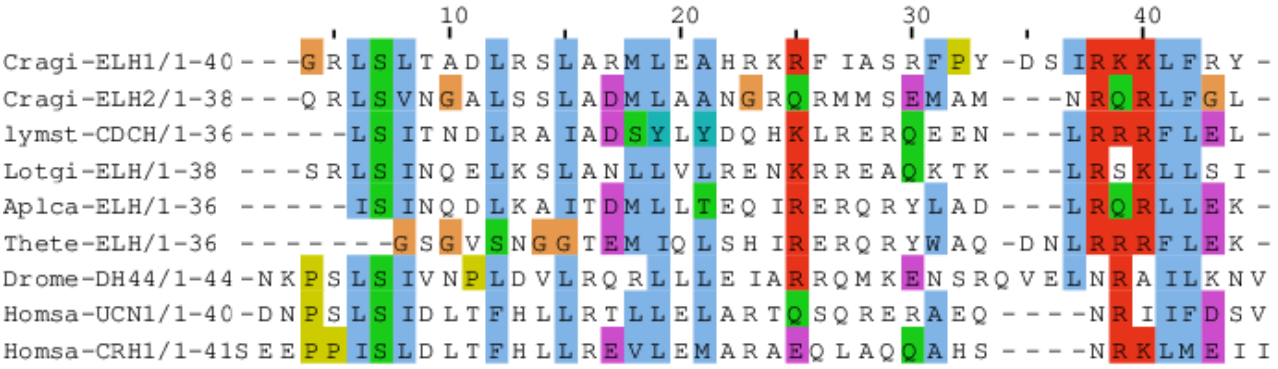

Figure 1: Multiple sequence alignment of Cragi-ELH and ELH-related family members. *Crassostrea gigas* predicted Cragi-ELH1 and Cragi-ELH2 (FQ667900.1) were aligned with sequences from mollusks: *Lymnaea stagnalis:* Lymst-CDCH (P06308); *Lottia gigantea*: Lotgi-ELH (V3YYG7); *Aplysia californica:* Aplca-ELH (P01362); annelids: *Theromyzon tessalum*: Thete-ELH (P80594.1); arthropods: *Drosophila melanogaster*: Drome-DH44 (Diuretic Hormone 44) (AAF54421.4) and vertebrates: *Homo sapiens*: Homsa-UCN (urocortin 1) (NP_003344.1) and Homsa-CRH1 (corticoliberin) (NP_000747.1). Conserved amino acids are highlighted.

A

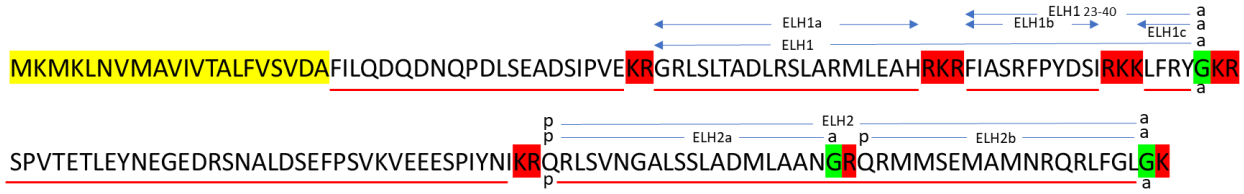

B

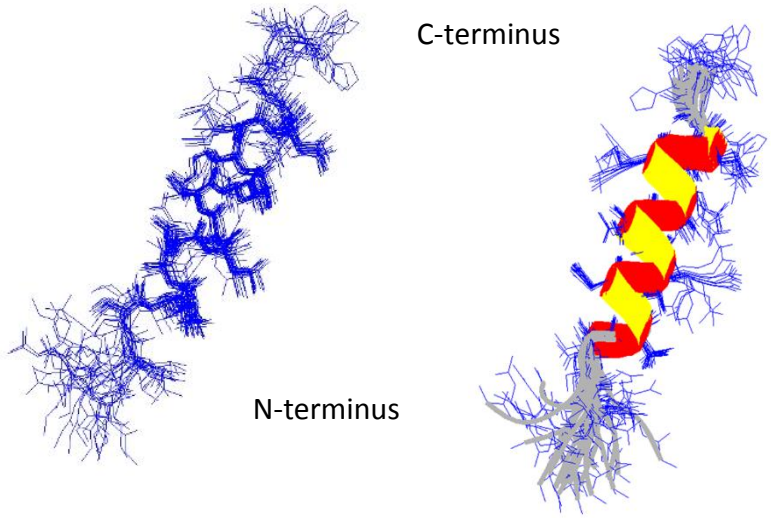

Figure 2: Structure of Cragi-ELH precursor and of some mature peptides. A: Amino acid sequence of *Crassostrea gigas* ELH precursor (Cragi-ELH). The predicted signal peptide is highlighted in yellow; the likely convertase processing sites are highlighted in red, the glycine residues likely to be converted into a C-terminal amide are highlighted in green, the mature neuropeptides detected by MS are underlined in red. The post-translational modifications: pyroglutamate (p) and C-terminal amide (a) are indicated. The various peptides synthesized are indicated in blue. B: Superimposition of the 18 lowest energy conformers of peptide Cragi-ELH1a in presence of deuterated DPC micelles, fitted on segment 4-17 backbone atoms (rmsd: 0.28) and ribbon representation of the structure.

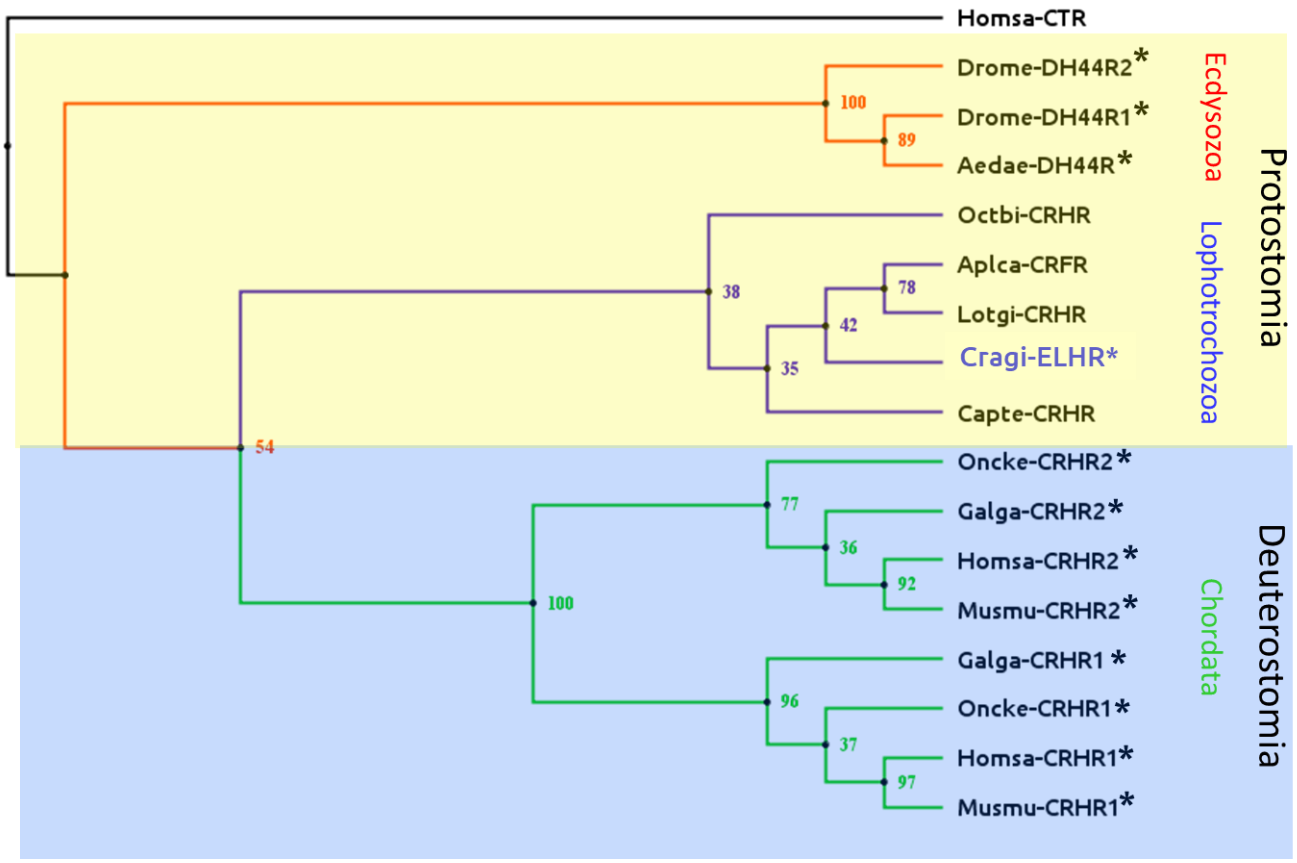

Figure 3: Phylogenetic representation of the relationship between Cragi-ELHRs and other ELHR family members. Phylogenetic and molecular evolutionary analyses were conducted using the maximum likelihood methods using the edited sequence alignment of the deduced receptor protein sequences obtained from Seaview. The accession numbers and the sequences used to construct the tree are: *Aedes aegypti*: Aedae-DH44R (QBC65449.1); *Aplysia californica*: Aplca-CRHR (XP_012938918.2); *Crassostrea gigas:* Cragi-ELHR* (CHOYP_CRHR.1.2, Gigaton); *Capitella telleta*: Capte-CAPTEDRAFT_93223 (ELU10073.1); *Drosophila melanogaster*: Drome-DH44R1* (AAF58250.1), Drome-DH44R2* (AAM68690.3); *Gallus gallus*: Galga-CRHR1* (NP_989652.1), Galga-CRHR2* (XP_015136531.2); *Homo sapiens*: Homsa-CRHR1* (NP_004373.2), Homsa-CRHR2* (NP_001874.2), Homsa-CTR* (calcitonin receptor) (NP_001733.1); *Lottia gigantea*: Lotgi-LOTGIDRAFT_141716 (XP_009049617.1); *Mus musculus*: Musmu-CRHR1* (NP_031788.1), Musmu-CRHR2* (NP_001275547.1); *Octopus*

bimaculoides: Octbi-CRHR-like (XP_014771477.1); *Oncorhynchus keta*: Oncke-CRHR1 (CAC81753.1), Oncke-CRHR2 (CAC81754.1). (*): functionally characterized receptors. Green branches correspond to vertebrate receptors, blue branches to lophotrochozoan (molluscs and annelids) receptors, red branches to ecdysozoan receptors. Branch node labels correspond to likelihood ratio test values.

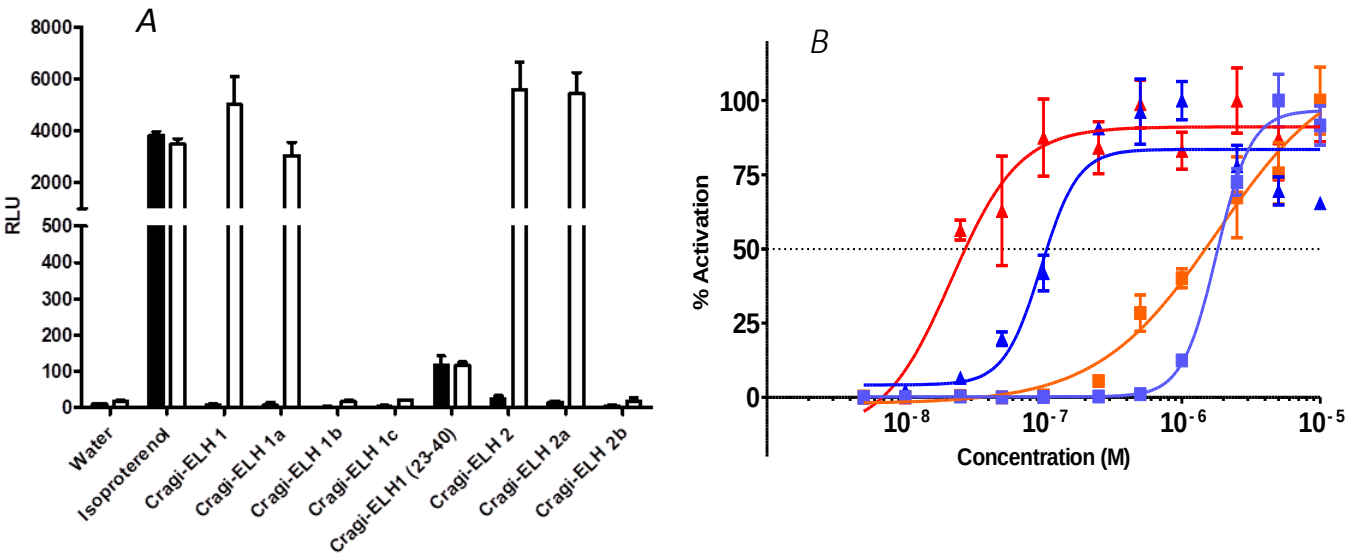

Figure 4: Activation modalities of Cragi-ELHR by Cragi-ELH peptides. A: Activation of *Crassostrea gigas* ELH receptor (Cragi-ELHR) by Cragi-ELH1 and CragiELH2 synthetic peptides at a concentration of 10^{-5}M (n=3). B: Dose-dependent effect of Cragi-ELH1 (▲) Cragi-ELH1a (■), Cragi-ELH2 (▲) and Cragi-ELH2a (■) on Cragi-ELHR expressed in HEK293T cells. Data are shown as relative (%) to the highest value (100% activation) and represent the mean of an experiment (n=3) performed in triplicate. Vertical bars represent the standard error of the mean (SEM). Black bar: empty plasmid, open bar: Cragi-ELHR plasmid.

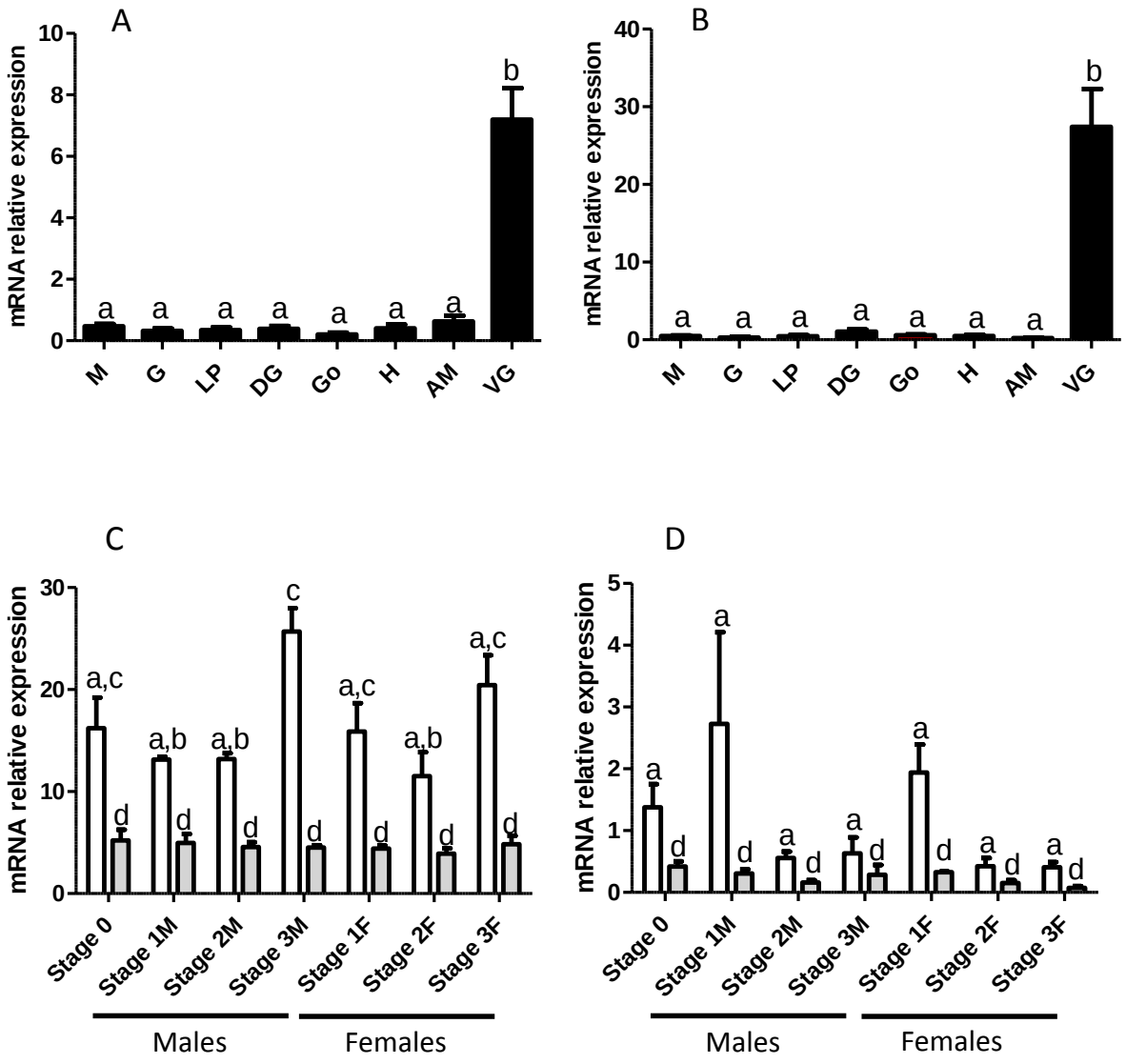

Figure 5: Expression of mRNAs encoding Cragi-ELHR and Cragi-ELH precursor in adult tissues. Distribution of mRNAs encoding Cragi-ELHR (A) and Cragi-ELH precursor (B) in adult tissues: M: Mantle (n=10); G: Gills (n=5); LP: Labial palps (n=5); DG: Digestive gland (n=5); Go: Gonad (mix of all stages) (n=5); H: Heart (n=10); AM: Adductor muscle (n=5); VG: Visceral ganglia (n=5). Distribution of mRNAs encoding Cragi-ELH (open bars) and Cragi-ELHR (grey bars) in the VG (C) and in the gonad (D) during gametogenesis: Stage 0: sexual resting stage; stage 1: gonial multiplication stage; stage 2: tubule development and maturation stage and stage 3: sexual maturity stage. Each value is the mean + SEM of at least 4 pools of 5 animals. Expression levels were normalized to Elongation Factor 1 α (EF1α) mRNA. Results were statistically tested with a

one-way ANOVA $p<0.05$. Vertical bars represent the standard error of the mean (SEM). Bars with different labels are statistically significantly different.

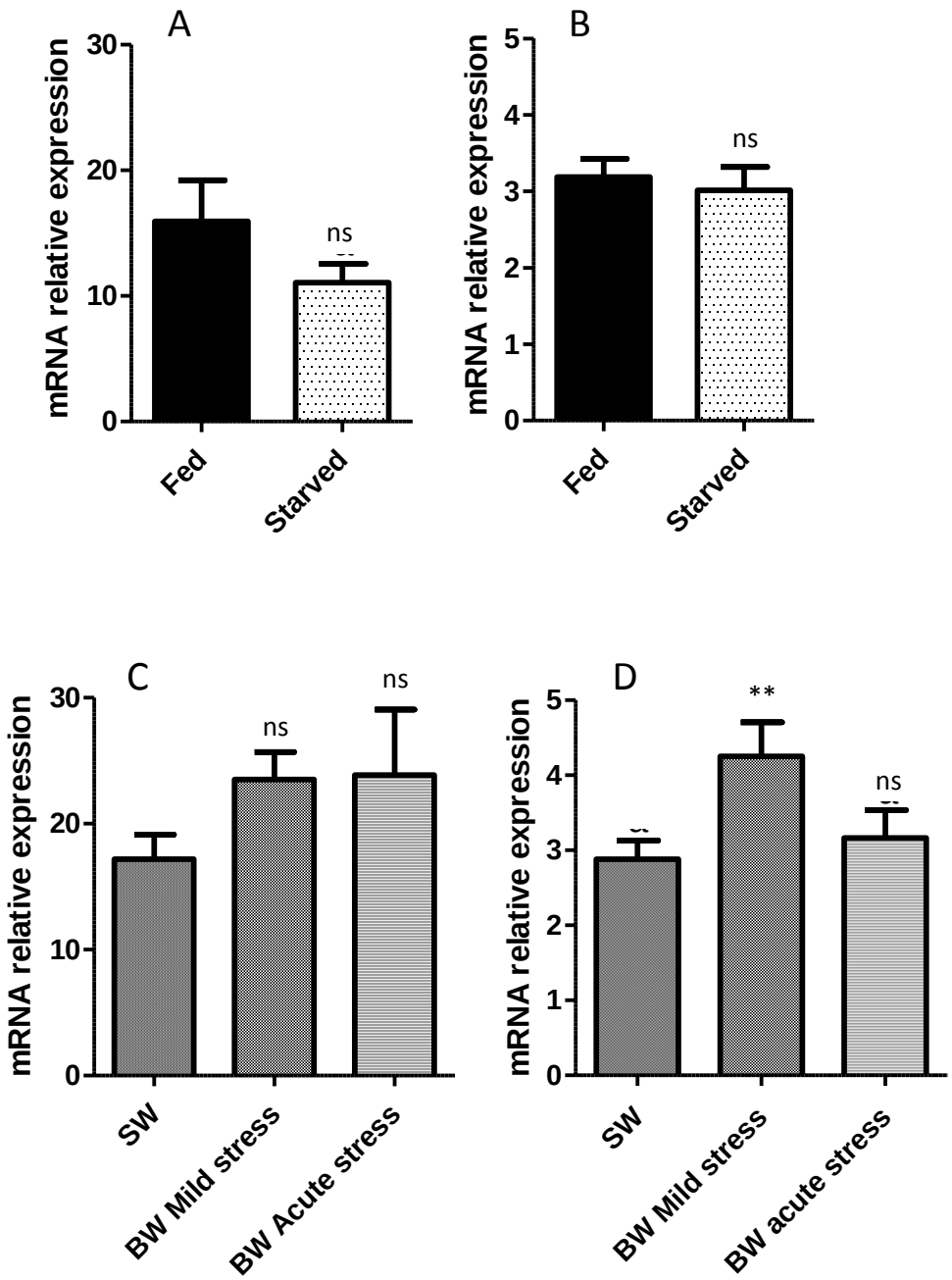

Figure 6: Expression of mRNAs Cragi-ELH precursor and Cragi-ELHR in VG of oysters after starvation and after a hyposaline stress. Expression of Cragi-ELH precursor (A) and Cragi-ELHR (B) in the VG of fed (n=13 and n=14) and starved oysters (n=14 and n=15). Expression of Cragi-ELH precursor (C) and Cragi-ELHR (D) in the VG of oysters acclimatized to brackish water. Each value is the mean + SEM of n=18 VG (SW), n=6 VG (BW Mild stress) and n=16 VG (BW acute stress). Expression levels were normalized to Elongation Factor 1α (EF1α) mRNA. Results were statistically tested with a Student's t test *p<0.05, **p<0.01, ns: non-

significant. Vertical bars represent the standard error of the mean (SEM). SW: Sea water, BW: Brackish water.